Convergence of the many-body expansion of interaction potentials: From van der Waals to covalent and metallic systems

Andreas Hermann, Robert P. Krawczyk, Matthias Lein, and Peter Schwerdtfeger*
Centre of Theoretical Chemistry, Physics and Institute of Advanced Studies and Institute of Fundamental Sciences, Massey University (Auckland Campus), Private Bag 102904, North Shore MSC, Auckland, New Zealand

I. P. Hamilton
Department of Chemistry, Wilfrid Laurier University, Waterloo, N2L 3C5, Canada

James J. P. Stewart
Stewart Computational Chemistry, 15210 Paddington Circle, Colorado Springs, Colorado, CO 80921, USA
(Received 1 May 2007; published 31 July 2007)

The many-body expansion of the interaction potential between atoms and molecules is analyzed in detail for different types of interactions involving up to seven atoms. Elementary clusters of Ar, Na, Si, and, in particular, Au are studied, using *first-principles* wave-function- and density-functional-based methods to obtain the individual n-body contributions to the interaction energies. With increasing atom number the many-body expansion converges rapidly only for long-range weak interactions. Large oscillatory behavior is observed for other types of interactions. This is consistent with the fact that Au clusters up to a certain size prefer planar structures over the more compact three-dimensional Lennard-Jones-type structures. Several Au model potentials and semiempirical PM6 theory are investigated for their ability to reproduce the quantum results. We further investigate small water clusters as prototypes of hydrogen-bonded systems. Here, the many-body expansion converges rapidly, reflecting the localized nature of the hydrogen bond and justifying the use of two-body potentials to describe water-water interactions. The question of whether electron correlation contributions can be successfully modeled by a many-body interaction potential is also addressed.

DOI: 10.1103/PhysRevA.76.013202 PACS number(s): 36.40.−c, 31.15.Ar, 31.15.Ew

I. INTRODUCTION

A wide variety of analytical two-body potentials is available for the interaction between atoms or molecules [1,2], the most successful and widely used being the Lennard-Jones (LJ) potential [3]. Despite the success of the LJ potential in simulating clusters, liquids, solids, and corresponding phase transitions, the question always arises whether higher-order energy contributions can be neglected—that is, whether the many-body expansion

$$E(N) = \sum_n E_n(N) = \sum_{i<j} E_{ij}(2) + \sum_{i<j<k} E_{ijk}(3) + \cdots \qquad (1)$$

converges rapidly. Here $E_n(N)$ are the individual n-body contributions in a cluster of N interacting subsystems.

It is well known that for interactions between rare gas atoms, the three-body term is relatively small—i.e., a few percent of the two-body term around the equilibrium distance for the rare gas trimer [4]. However, the number of three-body terms scales as N^3 whereas the two-body contributions scale as N^2. This implies that, for large clusters or solids, three-body contributions may be significant. For example, for the fcc solid phase of Ar, the cohesive energy changes from 692 to 645 cm^{-1} upon inclusion of the three-body term in Eq. (1) [5]. Three-body forces in rare-gas solids become especially important at short distances as in the high-pressure regime [6]. The scaling behavior also implies that each nth-order term in Eq. (1) should be at least one order of magnitude smaller than the corresponding (nth-1)-order term to assure convergence. While this is largely fulfilled for rare-gas atoms, it is highly questionable for other systems [4].

Two-body interactions like the LJ or Morse potential [7] favor compact cluster structures; i.e., they optimize the number of connections or bonds between atoms. For any physically sensible potential one therefore obtains an ideal triangle for the interaction between three atoms and an ideal tetrahedron for the interaction between four atoms. Jahn-Teller distortions, such as those found for Na_3, Au_3, and Au_4 [8], are direct evidence for the importance of three- or higher-body forces. Also, it is well known that for small Au clusters planar structures are energetically favored over the more compact three-dimensional (3D) structures [9]. This raises the question whether Au clusters can be adequately described by an n-body expansion with low n. An alternative would be to include all n-body forces in an effective many-body potential depending only on the pairwise atomic distances r_{ij} as in the Sutton-Chen [10,11] or Gupta [12] potential. However, while these potentials are commonly used for large clusters, their accuracy has so far not been addressed in detail.

This study is mainly concerned with Au clusters as the chemistry of gold has recently received increasing interest [13,14] due to the unexpected catalytic activity of Au nanoclusters [15–20] and, for example, its application to fuel cells [21,22] and biological [23–26] systems. Furthermore, Au shows remarkable differences compared to the lighter group-11 elements [27–29] due to large relativistic effects. Au atoms assemble in extraordinary structures, such as gold

*p.a.schwerdtfeger@massey.ac.nz

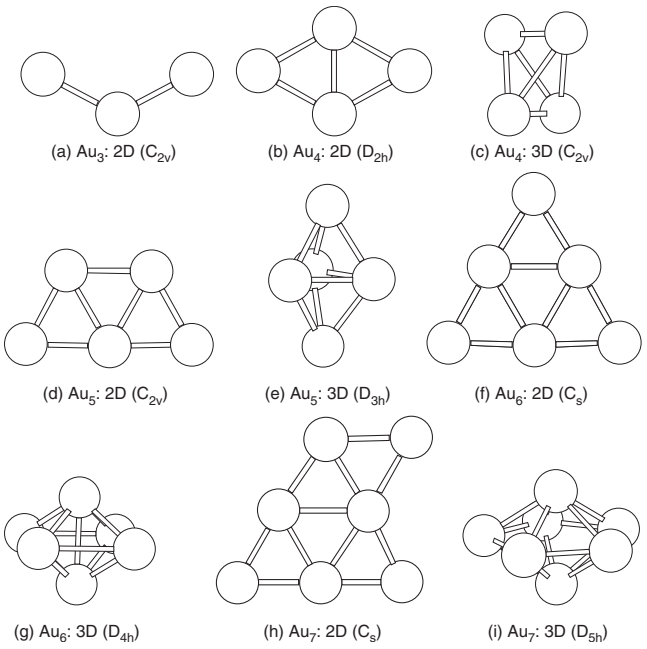

FIG. 1. Geometries of optimized 2D and 3D Au_N clusters ($N=3,\ldots,7$) used for many-body decomposition.

nanorods [30] and gold pyramids [31,32], and their correct description poses a formidable computational task. In order to efficiently predict the energetically favored structures, effective many-body potentials for Au have been developed [33–36]. It has been pointed out, however, that the convergence of the n-body expansion for gold is rather slow [8].

In this paper we analyze in detail the convergence of n-body expansions of the interaction potential for elementary Au clusters and address the performance of effective many-body potentials and a recently developed semiempirical parametrization. For comparison, we study elementary Ar, Na, and Si clusters as prototypes for van der Waals, metallic, and covalently bonded systems, as well as small water clusters as exemplary hydrogen-bonded systems. Water clusters are of specific interest due to the unique significance of water as a solvent, its inherent anomalous properties, and its generally important role in chemistry, biology, and physics. For both atomic and molecular clusters, we investigate the contribution of n-body terms to the total energy and also to the electron correlation energy.

II. COMPUTATIONAL DETAILS

The decomposition of the interaction energy is done following Kaplan *et al.* [37]. The total energy of a system of N atomic or molecular units can be represented as a finite sum

$$E(N) = \sum_{n=1}^{N} E_n(N). \tag{2}$$

The terms $E_n(N)$ are the n-body energy term of the N-particle system with $\max(n)=N$. In a recursive definition they are given by

$$E_1(N) = \sum_{a=1}^{N} E(a) \tag{3}$$

and

$$E_2(N) = \sum_{a<b}^{\{N\}} \varepsilon_{ab}, \tag{4}$$

where

$$\varepsilon_{ab} = E(ab) - [E(a) + E(b)] = E(ab) - E_1(ab). \tag{5}$$

The sum in Eq. (3) is taken over the energies of all N units of the system, and the sum in Eq. (4) is taken over the two-body interaction energies ε_{ab} of all $\frac{N(N-1)}{2}$ different pairs of particles. For the definition of the higher-order terms see Kaplan *et al.* [37]. A closed formula can be derived which can be implemented in a more convenient form. Here the n-body energies are written as [37]

$$E_2(N) = \sum_{a<b}^{\{N\}} E(ab) - a_{2N}^1 E_1(N), \tag{6a}$$

$$E_3(N) = \sum_{a<b<c}^{\{N\}} E(abc) - a_{3N}^1 E_1(N) - a_{3N}^2 E_2(N), \tag{6b}$$

$$E_4(N) = \sum_{a<b<c<d}^{\{N\}} E(abcd) - a_{4N}^1 E_1(N) - a_{4N}^2 E_2(N) - a_{4N}^3 E_3(N), \tag{6c}$$

where

$$a_{mn}^k = \binom{n-k}{m-k} = \frac{(n-k)!}{(n-m)!\,(m-k)!}. \tag{7}$$

A program for the automatic n-body decomposition of arbitrary structures has been developed in our group.

We consider clusters of up to seven atoms. This cluster size allows us to observe the importance of higher than three-body effects and, for 3D clusters, goes beyond the compact octahedral structure. Three- and partly four-body contributions have already been discussed to some extent in the literature [4]. We choose three prototype cluster structures: a linear structure, a planar structure, and the well-known LJ type structure. These structures permit us to observe the convergence of the many-body expansion for 1D, 2D, and 3D clusters (the corresponding point groups are $D_{\infty h}$ for the 1D, C_s for the 2D, and, for $N=7$, D_{5h} for the 3D structure). Literature-known LJ and gold-cluster geometries [9,38–41] were chosen as starting points, and all geometries were optimized for the linear, planar, and LJ-type cases. The geometry optimizations were performed [42] at the *ab initio* level using second-order many-body perturbation theory (MP2) and coupled-cluster singles-doubles (triple) [CCSD(T)] theory and at the density functional theory (DFT) level using the local density approximation (LDA) [43]. However, for some specific examples we also used the (hybrid) generalized gradient approximation (GGA) functionals Becke three-

TABLE I. $(Ar,Au,Na,Si,H_2O)_7$ clusters: binding energies and many-body energy contributions. The binding energies E_b are given in eV/atom; the n-body contributions $E_n(N)$ are normalized to the largest contribution. $D_{\infty h}$: 1D linear chain. C_s: planar geometry (2D). D_{5h}: 3D geometry. See text and Figs. 1 and 2 for a detailed description of geometries.

Geometry	Method	E_b	E_2	E_3	E_4	E_5	E_6	E_7
					Ar			
1D ($D_{\infty h}$)	LDA	0.031	−1.0000	−0.5914	0.7510	−0.5229	0.1812	−0.0205
	MP2	0.012	−1.0000	−0.0245	−0.0041	−0.0006	−0.0001	0.0000
2D (C_s)	LDA	0.050	−1.0000	−0.0811	0.2040	−0.1349	0.0676	−0.0253
	MP2	0.023	−1.0000	−0.0128	0.0021	0.0028	−0.0005	−0.0000
3D (D_{5h})	LDA	0.067	−1.0000	0.1552	−0.1078	0.1644	−0.1016	0.0255
	MP2	0.033	−1.0000	−0.0018	−0.0206	0.0105	−0.0049	0.0008
					Au			
1D ($D_{\infty h}$)	LDA	1.770	−0.0683	−0.0503	0.4180	−0.9586	1.0000	−0.4023
	MP2	1.146	−0.3532	−0.1229	0.6553	−1.0000	0.7565	−0.1908
2D (C_s)	LDA	2.405	−0.5824	0.5782	−0.2728	−0.6908	1.0000	−0.3684
	MP2	2.040	−0.1725	−0.3025	0.8541	−1.0000	0.5220	−0.0865
3D (D_{5h})	LDA	2.407	−0.4565	0.7468	−1.0000	0.8312	−0.3961	0.0891
	MP2	2.128	−0.6549	0.7517	−0.9623	1.0000	−0.7179	0.2308
					Na			
1D ($D_{\infty h}$)	LDA	0.411	0.0170	−0.1911	0.5891	−1.0000	0.8165	−0.2503
	MP2	0.133	−0.1386	0.5460	−1.0000	0.7886	−0.1871	−0.0392
2D (C_s)	LDA	0.556	−0.0753	−0.1741	0.6369	−1.0000	0.7389	−0.2071
	MP2	0.276	0.0553	−0.3723	0.8314	−1.0000	0.6078	−0.1454
3D (D_{5h})	LDA	0.645	−0.7013	0.9920	−1.0000	0.1901	0.3596	−0.1927
	MP2	0.376	0.0035	−0.3733	0.8045	−1.0000	0.6185	−0.1547
					Si			
1D ($D_{\infty h}$)	LDA	2.808	−0.0091	0.2153	−0.7715	1.0000	−0.5484	0.1023
	MP2	1.734	−0.0795	0.0750	0.3960	−1.0000	0.8368	−0.2416
2D (C_s)	LDA	3.397	−0.4440	0.1433	0.4156	−1.0000	0.8624	−0.2694
	MP2	2.212	−0.1250	0.3228	−0.8067	1.0000	−0.6004	0.1369
3D (D_{5h})	LDA	3.486	−0.6601	0.6942	−0.7044	0.9952	−1.0000	0.3739
	MP2	2.295	−0.4178	0.3283	−0.5534	1.0000	−0.9672	0.3454
					H_2O			
1D (chain)	LDA	0.394	−1.0000	−0.0999	−0.1312	0.0873	−0.0115	−0.0041
	PW91	0.250	−1.0000	−0.1849	−0.0450	0.0296	−0.0157	0.0112
	MP2	0.241	−1.0000	−0.2198	−0.0155	−0.0005	−0.0001	0.0000
2D ($R5$)	LDA	0.635	−1.0000	−0.2031	−0.1712	0.1933	−0.0925	0.0135
	PW91	0.419	−1.0000	−0.3247	−0.0399	−0.0389	0.0194	0.0007
	MP2	0.400	−1.0000	−0.3753	−0.0502	0.0019	−0.0002	0.0001
3D (C)	LDA	0.655	−1.0000	−0.1771	−0.0641	0.0936	−0.0531	0.0076
	PW91	0.418	−1.0000	−0.1679	−0.0996	−0.0073	0.0260	−0.0077
	MP2	0.413	−1.0000	−0.3085	−0.0317	0.0046	−0.0012	0.0002

parameter Lee-Yang-Parr (B3LYP) [44] and PW91 [45]. In particular, water clusters were optimized at the DFT-PW91/augmented correlation-consistent polarization, valence triple zeta (aug-cc-pVTZ) level, as this functional reasonably describes hydrogen-bonded systems [46].

To describe the weak interactions in the Ar clusters an aug-cc-pVTZ basis set was used [47]. For Na and Si, we used the scalar relativistic pseudopotentials (PPs) of Hay and Wadt [48] with the accompanying double-zeta basis sets. Tests with a cc-pVTZ basis set gave only small deviations for the n-body terms. For Au we used a small-core scalar relativistic PP from the Stuttgart group [49] together with a contracted $(7s5p5d3f)/[5s3p3d1f]$ basis set. Selected geometries of optimized Au_N clusters $(N=3,\ldots,7)$ are shown in

TABLE II. Compressed Ar_7 clusters (see text): binding energies and many-body energy contributions. The binding energies E_b are given in eV/atom; the n-body contributions $E_n(N)$ are normalized to the largest contribution.

Geometry	Method	E_b	E_2	E_3	E_4	E_5	E_6	E_7
1D ($D_{\infty h}$)	LDA	0.028	−0.8581	−0.0212	0.4492	−1.0000	0.8008	−0.2227
	MP2	−0.006	1.0000	−0.0644	−0.0072	0.0013	0.0009	0.0001
2D (C_s)	LDA	0.050	−1.0000	0.1860	−0.0375	−0.1953	0.2479	−0.0902
	MP2	0.006	−1.0000	−0.2359	0.0056	0.0281	−0.0079	0.0002
3D (D_{5h})	LDA	0.066	−1.0000	0.3443	−0.4618	0.4624	−0.2276	0.0453
	MP2	0.024	−1.0000	−0.0452	−0.0466	0.0291	−0.0124	0.0020

Fig. 1. The geometries of the optimized Na_7 and Si_7 clusters are very similar to those of Au_7. For the Si clusters, the spin triplet states have been chosen.

III. DECOMPOSITION OF THE CLUSTER ENERGIES

The binding energies and the many-body decomposition of the interaction energies for the elementary clusters of seven atoms (or molecules in the case of H_2O) are listed in Table I. For better comparison, the n-body contributions are normalized to the largest respective component.

The minimum geometry of the Ar cluster is known to be the compact 3D (LJ-type) structure [5]. The planar and linear structures represent only local minima on the potential hypersurface and lie much higher in energy. Both LDA and MP2 calculations confirm this trend. They also demonstrate clearly that Ar tries to maximize the interaction between single atoms: the two-body terms are generally dominant and the n-body decomposition converges fast. The sole exception is the linear Ar_7 chain calculated in the LDA, which has significant many-body contributions E_n up to $n=5$. However, it is well known that, for example, three-body forces become important if solid Ar is put under pressure—that is, if one enters the repulsive region of the energy hypersurface [50]. Thus, we also performed a n-body decomposition for compressed Ar_7 clusters, obtained by scaling the optimized Au_7 structures by the ratio a_{Ar}/a_{Au} of the solid-state lattice constants for Ar and Au. These clusters' bond lengths are on average about 10% smaller than in the optimized structures, and the n-body decompositions (see Table II) contain much larger higher contributions. LDA results especially show an erratic behavior, highlighting the question of its applicability in the high-pressure regime. The successful development of density functionals for long-range interactions such as dispersion forces could be rigorously tested by comparing the n-body contributions to those of more accurate wave-function-based theories.

The question arises whether electron correlation can be treated by a many-body decomposition, as has been suggested for the rare gases and mercury [51]. We therefore separate the interaction energy in our MP2 calculation into a Hartree-Fock (HF) part E^{HF} and an electron correlation part E^c. Table III shows the very smooth and fast convergence of the correlation energy in the case of Ar_7 clusters. For such van der Waals–bonded systems the n-body decomposition of the correlation energy converges even faster than the total interaction energy (see Table I). Hence, for an accurate simulation of larger rare-gas clusters or the solid state one may take the HF total electronic energy and add the two-body electron correlation term [52]. It would be of interest to test if this technique is also applicable to the high-pressure regime of solid Ar.

For Si_7, Na_7, and Au_7 the compact 3D structure is most stable; see Table I. For example, the Si cluster with the lowest energy is the pentagonal bipyramid in agreement with literature [53–55]. However, for Au the 3D structure is lowest in energy only by a very small margin, especially for the LDA calculation. This is in contrast to earlier findings of Bonacić-Koutecký *et al.* [56] but in agreement with Wang *et al.* [40]. The energetic order of the structures depends strongly on the functional used. For example, using the B3LYP (or PW91) functional and our basis set, the optimized planar Au_7 structure is 0.739 eV (0.717 eV) lower in energy than the D_{5h} 3D structure. Similar results were also obtained by Walker [38]. It is clear that the LDA is not capable of describing the relative energetic order in Au clusters. In contrast to Ar the strong binding in the other elementary clusters shows comparable results for both the DFT and MP2 calculations. However, there are still deviations in the individual energy contributions in the n-body expansion; see Fig. 4 for a graphical representation of the Au cluster n-body terms. In general, the convergence behavior is very poor for Si, Na, and Au and large oscillations are found both in the DFT and MP2 results. Note that the most important contribution for

TABLE III. Ar_7 clusters: correlation energies and their many-body expansion. E^c given in eV/atom, $E_n(N)$ normalized to the largest component.

Geometry	E^c	E_2	E_3	E_4	E_5	E_6	E_7
1D ($D_{\infty h}$)	0.022	−1.0000	−0.0121	−0.0010	0.0001	0.0001	0.0000
2D (C_s)	0.040	−1.0000	−0.0010	0.0008	0.0012	−0.0003	0.0000
3D (D_{5h})	0.058	−1.0000	0.0100	−0.0086	0.0044	−0.0021	0.0004

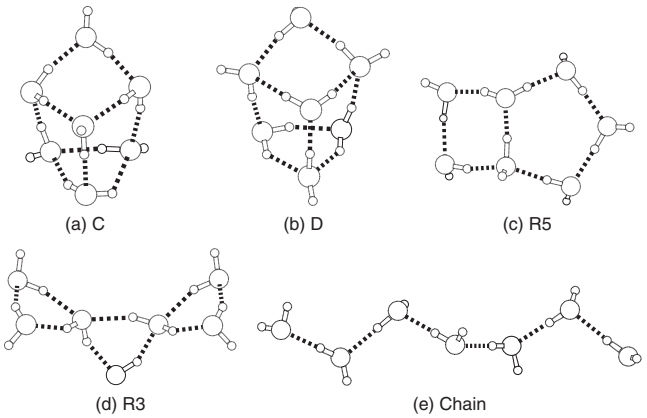

FIG. 2. Selected geometries of optimized $(H_2O)_7$ clusters.

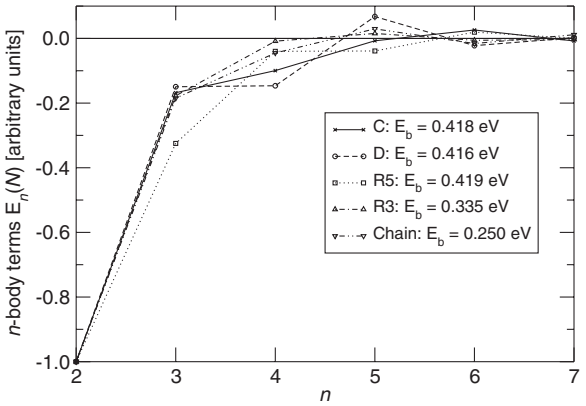

FIG. 3. $(H_2O)_7$ clusters: normalized n-body expansion of interaction energies from DFT-PW91 calculations. E_b is the binding energy per molecule. See text and Fig. 2 for a description of structures.

many structures is the five-body term. The three-body terms, which were of minor importance for Ar, are here of similar size as the two-body terms. Interestingly, the Na clusters have much in common with the Au clusters. They have the smallest two-body contribution (with the single exception of the LDA result for the 3D cluster). The five-body terms usually provide the highest contribution to the total cluster energy. Similar to Na, the linear Si_7 cluster has the lowest two-body contribution and large five-body terms. The six-body terms are also very large, and in the case of the LDA calculations they are even larger than the five-body terms. The seven-body terms are mostly repulsive. Only two clusters (the planar cluster at the LDA level and the linear cluster at the MP2 level) have negative seven-body contributions to the cluster energy. Interestingly, for Si_7, the energy difference between the global minimum and the planar structure is between 0.47 eV and 0.62 eV (PW91, 0.47 eV; MP2, 0.58 eV; LDA, 0.62 eV). This is quite low in comparison to other published Si minimum-energy structures; e.g., a capped tetrahedron lies 0.65 eV above the global minimum [54]. The results clearly demonstrate that the convergence behavior of the n-body expansion is very poor as well.

IV. MOLECULAR TEST CASE: WATER

The preceding section has shown that bound atomic systems can have significant higher-order terms in the n-body expansion. The question remains whether molecular systems show similar behavior. This is of special interest since many calculations of molecular systems are performed using model potentials to describe molecular interactions [57]. Many of these potentials fit a model two-body interaction to experimental or accurate *ab initio* data such as, for example, for H_2O clusters. Therefore, an analogous many-body decomposition has been performed for $(H_2O)_N$ clusters for $N=7$. Previous studies have used water clusters up to $N=5$ to compare the performance of several model potentials with MP2/aug-cc-pVDZ calculations [58] and found a rapid decrease of higher-order contributions, in generally satisfactory agreement with *ab initio* and model potential calculations.

Structures for water heptamer clusters were thoroughly investigated by Kim *et al.* [59]. Selected geometries of optimized $(H_2O)_7$ clusters are shown in Fig. 2. We chose the lowest-energy compact structures (cagelike *C* and *D*) and the lowest-energy planar structure (*R*5). Additionally, we investigated a linear chain of seven water molecules and a planar three-ring structure (*R*3). All geometries except for the linear chain were optimized prior to the many-body decomposition. The latter would upon optimization change towards the *R*3 structure.

Table I lists the n-body energy decomposition for exemplary 1D (chain geometry), 2D (*R*5), and 3D water clusters (*C*). Additionally, Fig. 3 compares the n-body decomposition of all clusters and the binding energy E_b per molecule for each structure, calculated at the DFT-PW91 level.

We first note the generally good agreement between the DFT-PW91 and MP2 calculations (see Table I), illustrating the usefulness of the PW91 functional for such hydrogen-bonded systems. DFT-LDA calculations, as expected, tend to overbind, but are in basically good agreement with the other methods. In contrast to Au, Na, and Si, the n-body decomposition converges quickly for water, although not as quickly as for Ar. The three-body terms are only about 20% of the

TABLE IV. $(H_2O)_7$ clusters: correlation energies and their many-body expansion. E^c given in eV/molecule, $E_n(N)$ normalized to the largest component.

Geometry	E^c	E_2	E_3	E_4	E_5	E_6	E_7
1D (chain)	0.087	−1.0000	0.0000	−0.0045	−0.0001	−0.0002	0.0000
2D (*R*5)	0.133	−1.0000	0.0253	−0.0201	0.0050	−0.0009	0.0002
3D (*C*)	0.146	−1.0000	0.0195	−0.0223	0.0100	−0.0026	0.0004

two-body terms, and higher-order terms are even less important. Interestingly, the two-, three-, and four-body terms are all attractive. For some clusters even the five-body terms are attractive. Furthermore, there is no strong dependence on the cluster geometry; 1D, 2D, and 3D structures show very similar behavior. This illustrates the local nature of the hydrogen bond in water.

Using our MP2 calculations, we decomposed the total energy into the Hartree-Fock part E^{HF} and the correlation part E^c in the same way as for the Ar clusters. We then studied the many-body decomposition of E^c only, as shown in Table IV. For all water clusters, the correlation energy E^c converges at least one order of magnitude faster than the total energy. Thus, it should be possible to describe E^c in aqueous systems by adding a two-body model potential to the Hartree-Fock energy E^{HF}. Once parametrized, this should pave the way to affordable yet accurate cluster or solid-state calculations. However, from Table I it can be concluded that a decomposition of the total energy in n-body terms is also meaningful and can be truncated even after the two-body term without large error. This justifies the construction of empirical model potentials and explains their success in modeling aqueous systems at ambient conditions.

V. SPECIAL CASE OF GOLD

Since the simulation of large Au clusters is our main interest, we further investigated the convergence behavior of the n-body expansion in these systems. Figures 4(a) and 4(b) show the decomposition of the interaction energy for Au_7 clusters using MP2 and LDA calculations, respectively. It can be seen that the LJ-type 3D cluster shows a different decomposition behavior than the planar and linear structures. The former has alternating signs for all n-body terms, whereas for the latter both three- and four-body terms have the same sign in the MP2 calculation. For the planar and linear structures, the LDA results are quite different. Nevertheless, we observe a large oscillatory behavior and the convergence is extremely slow. Hence, for simulating large Au clusters, a many-body atomic decomposition of the total electronic energy is not advisable.

As expected, the situation is very similar for the smaller Au clusters as the n-body decomposition for the Au_N ($N=3,\ldots,6$) shows (see Table V). For $N=4$ the largest energy contributions stem from the two-body interactions. In contrast, for the larger clusters higher-order n-body terms become important. Again the LDA and MP2 give quite different results. The n-body decomposition of the planar Au structures with three to seven gold atoms at the MP2 level of theory is given in Fig. 5. It can be seen that even for the smallest Au clusters, the n-body expansion does not converge smoothly. The planar Au_4 rhombus [Fig. 1(b)] and the planar Au_5 [Fig. 1(d)] structures have the same magnitude for the three- and four-body terms, but opposite signs.

In Table VI, the many-body expansion of the electron correlation energy of Au_N clusters ($N=3,\ldots,7$) is given. It clearly shows that the correlation energy does not converge smoothly. On the contrary, except for the smallest clusters ($N=3$), the $(N-2)$-body correlation term $E^c_{N-2}(N)$ generally has the largest magnitude. An oscillatory behavior for $E^c_n(N)$ has been found earlier in studies of the metal clusters Be_N and Li_N [60]. In contrast to the expansion of the interaction energy (see Fig. 4), where large differences for the different structure types were found, the behavior of the correlation energy is nearly independent of the structure, as shown in Fig. 6 for the Au_7 clusters. This suggests that a different decomposition scheme—for example, into molecular Au_2 units as suggested recently by Stoll [61]—might be faster converging. The two-body terms are the only exception as these show only slight variations in the cluster structure: the more compact the structure, the greater the relative importance of the two-body terms.

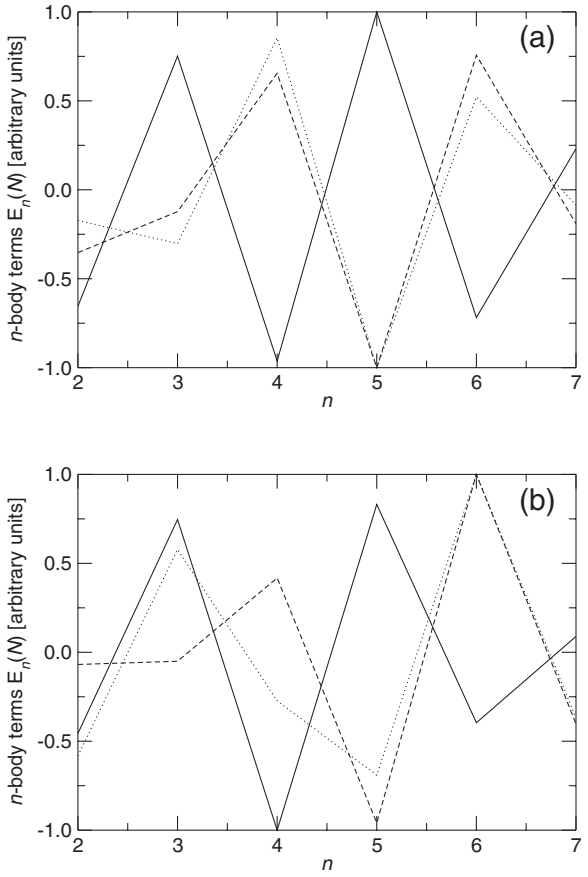

FIG. 4. Au_7 clusters: n-body expansion of the interaction energy. (a) MP2 results, (b) LDA results. Solid line: D_{5h} (3D). Dotted line: C_s (2D). Dashed line: $D_{\infty h}$ (1D). Energy terms are normalized to the largest respective component.

The question arises whether other schemes could correctly model Au clusters (and eventually solid states). As the many-body expansion can be applied to all common model potentials which may include higher-order contributions, we investigated the performance of the following known Au potentials: the two- and three-body Murrell-Mottram potentials as parametrized by Cox *et al.* [36,62] for the coinage metals, the Gupta potential with parameters taken from Wilson *et al.* [63,64], the Sutton-Chen potential as parametrized by Doye and Wales [35], and the Glue potential, defined and parametrized by Ercolessi *et al.* [33]. The Lennard-Jones potential parametrized by Erkoç and Katircioğlu [65] is also used for

TABLE V. Au_N clusters ($N=3,\ldots,6$): binding energies E_b and many-body energy contributions. E_b given in eV/atom; n-body contributions $E_n(N)$ are normalized to the largest respective component. For $N=7$ see Table I. See text and Fig. 1 for details.

N	Geometry	Method	E_b	E_2	E_3	E_4	E_5	E_6
3	1D ($D_{\infty h}$)	LDA	1.487	−1.0000	−0.1960			
		MP2	0.314	0.3727	−1.0000			
	2D (C_{2v})	LDA	1.526	−1.0000	0.1947			
		MP2	1.131	−1.0000	0.0927			
4	1D ($D_{\infty h}$)	LDA	1.652	−1.0000	0.1675	0.0011		
		MP2	0.351	0.3721	−1.0000	0.5248		
	2D (D_{2h})	LDA	1.980	−1.0000	0.7053	−0.2862		
		MP2	1.620	−1.0000	0.6401	0.3013		
	3D (C_{2v})	LDA	1.679	−1.0000	0.7855	−0.2515		
		MP2	0.228	−1.0000	0.3520	0.2496		
5	1D ($D_{\infty h}$)	LDA	1.631	−1.0000	0.0300	0.2591	−0.0831	
		MP2	1.253	−0.3247	−0.7180	1.0000	−0.4018	
	2D (C_{2v})	LDA	2.160	−1.0000	0.9073	−0.7801	0.3027	
		MP2	1.777	−1.0000	0.5047	−0.5042	0.2650	
	3D (D_{3h})	LDA	1.927	−0.9128	1.0000	−0.5284	0.0590	
		MP2	1.581	−0.9663	1.0000	−0.6255	0.1354	
6	1D ($D_{\infty h}$)	LDA	1.749	−0.5058	0.1549	0.8224	−1.0000	0.3939
		MP2	1.343	−0.2165	−0.4586	1.0000	−0.8710	0.2823
	2D (C_s)	LDA	2.433	−1.0000	0.9426	−0.7285	0.1173	0.0642
		MP2	2.109	−0.9594	−0.3192	1.0000	−0.7233	0.0761
	3D (D_{4h})	LDA	2.171	−0.7499	1.0000	−0.7752	0.1795	0.0290
		MP2	1.511	−0.8489	1.0000	−0.9392	0.6418	−0.2076

comparison but this represents a trivial case because only two-body forces are active and only compact LJ-type structures are obtained. In addition, the semiempirical PM6 method of Stewart [66], as implemented very recently in the MOPAC program package [67], was included in our investigation.

Figure 7 shows the many-body decomposition of a 3D compact, a 2D planar, and a 1D linear Au_7 cluster in comparison to the MP2 results. As anticipated, the Lennard-Jones and the Murrell-Mottram potential only have two- and three-body terms, respectively, and as a trivial consequence both methods fail to reproduce the many-body expansion of the reference MP2 calculation. Moreover, the three-body term for the planar structure is incorrectly described by the Murrell-Mottram potential. The Sutton-Chen and Gupta potentials show slightly improved performance for the 3D case, but both potentials converge too quickly with increasing n. Even more disturbingly, the performance of these potentials is less than satisfactory for the 2D and 1D cases. There is also a strong correlation of the convergence behavior with the dimensionality of the structure; i.e., going from 3D to 2D and finally to 1D improves the convergence. A comparison of the formulae of the Sutton-Chen potential

$$V = \varepsilon \sum_{i=1}^{N} \left(\frac{1}{2} \sum_{j \neq i}^{N} V_{ij} + c\sqrt{\rho_i} \right), \tag{8a}$$

$$V_{ij} = \left(\frac{\sigma}{r_{ij}} \right)^n, \tag{8b}$$

$$\rho_i = \sum_{j \neq i} \left(\frac{\sigma}{r_{ij}} \right)^m, \tag{8c}$$

and the Gupta potential

$$V = \sum_{i=1}^{N} \left(\sum_{j \neq i}^{N} V_{ij}(r_{ij}) + \sqrt{\sum_{j \neq i}^{N} W_{ij}(r_{ij})} \right), \tag{9a}$$

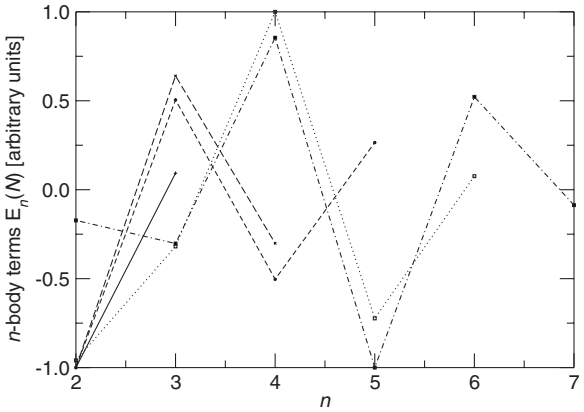

FIG. 5. Planar Au_N clusters ($N=3,\ldots,7$): MP2 n-body expansion of interaction energies. Energy terms are normalized to the largest component. Solid line: Au_3 triangle. Long-dashed line: Au_4 rhombus. Short-dashed line: Au_5 planar C_{2v}. Dotted line: planar Au_6 triangle. Dash-dotted line: planar Au_7 structure.

TABLE VI. Au_N clusters ($N=3,\ldots,7$): correlation energies and their many-body expansion from MP2 calculations. E^c given in eV/atom. The n-body contributions are normalized to the largest respective component. See text and Fig. 1 for details.

N	Geometry	E^c	E_2	E_3	E_4	E_5	E_6	E_7
3	1D ($D_{\infty h}$)	0.770	−1.0000	0.3892				
	2D (C_{2v})	0.894	−1.0000	0.3018				
4	1D ($D_{\infty h}$)	0.920	−0.8798	1.0000	−0.5013			
	2D (D_{2h})	1.230	−1.0000	0.6817	−0.3265			
	3D (C_{2v})	1.070	−1.0000	0.6913	−0.3482			
5	1D ($D_{\infty h}$)	1.031	−0.4852	0.9478	−1.0000	0.3867		
	2D (C_{2v})	1.307	−0.9147	1.0000	−0.9683	0.3869		
	3D (D_{3h})	1.368	−0.9740	1.0000	−0.9691	0.3793		
6	1D ($D_{\infty h}$)	1.074	−0.1965	0.5996	−1.0000	0.8165	−0.2626	
	2D (C_s)	1.488	−0.3816	0.6387	−1.0000	0.8272	−0.2797	
	3D (D_{4h})	1.637	−0.4514	0.6582	−1.0000	0.8316	−0.2978	
7	1D ($D_{\infty h}$)	1.151	−0.0876	0.3571	−0.8043	1.0000	−0.6563	0.1765
	2D (C_s)	1.485	−0.1654	0.3917	−0.8209	1.0000	−0.6626	0.1867
	3D (D_{5h})	1.736	−0.2274	0.4161	−0.8240	1.0000	−0.6793	0.1965

$$V_{ij} = A \exp[-p(r_{ij}/r_0 - 1)], \tag{9b}$$

$$W_{ij} = \zeta^2 \exp[-2q(r_{ij}/r_0 - 1)], \tag{9c}$$

shows their similarity and explains the analogous results of their n-body expansions as seen in Fig. 7. The Glue potential has slower convergence and shows the same behavior regardless of the structure of the cluster. Although this is in better agreement with the reference results for the linear and planar structures, it fails completely in describing the compact 3D LJ-type structure. We therefore conclude that none of the empirical many-body potentials is capable of producing accurate cluster structures, which is a rather unsatisfying situation.

Finally, let us move to the recently developed semiempirical PM6 approximation which should include all major many-body contributions if correctly parametrized. Indeed, the PM6 method gives the best overall agreement with the reference calculations. The expansions for the linear and pla-

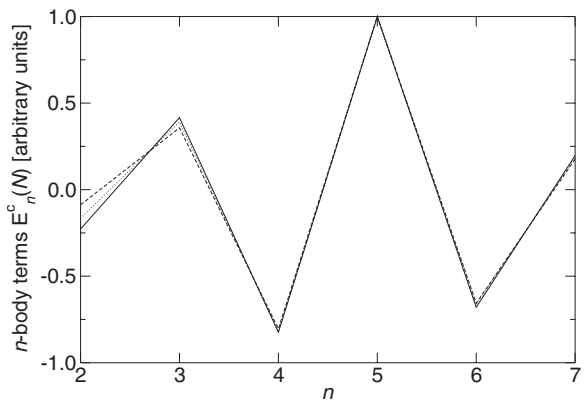

FIG. 6. Au_7 clusters: n-body expansion of the correlation energy E^c. Energy terms are normalized to the largest respective component. Solid line: D_{5h}. Dotted line: C_s. Dashed line: $D_{\infty h}$.

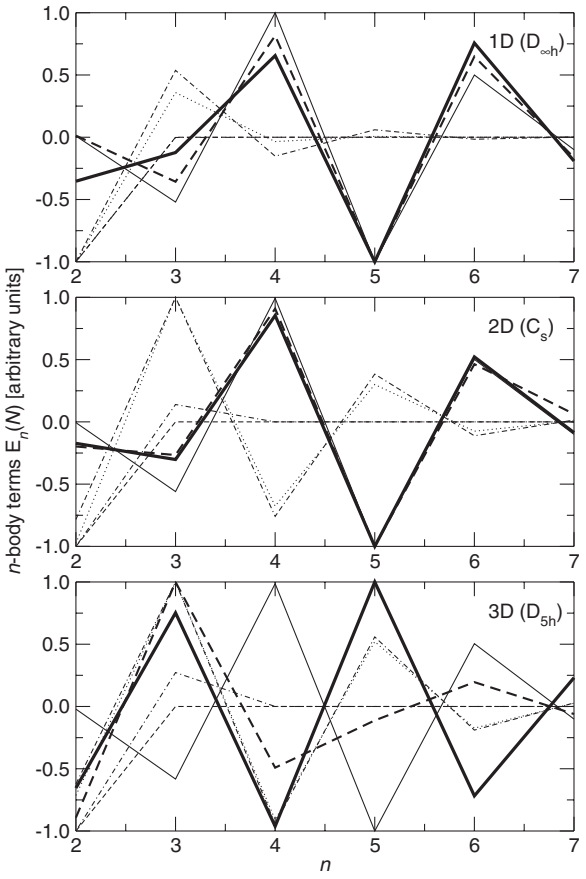

FIG. 7. Au_7 clusters: n-body expansion of interaction energies from different model potentials. From top to bottom: 1D ($D_{\infty h}$), 2D (C_s), 3D (D_{5h}). Energy terms are normalized to the largest respective component. Reference calculation: MP2 (thick solid line). Model potentials used: Lennard-Jones (dashed line), Murrell-Mottram (dash-dotted line), Gupta (dotted line), Sutton-Chen (double-dash–dotted line), Glue (solid line); PM6 method (thick dashed line).

nar structures are both in very good agreement with the MP2 results, and the expansion for the LJ-type structure agrees extremely well up to the four-body term with small deviations for the higher-order terms. Hence, this method could become very useful for (pre)optimizing larger Au clusters and in the search for candidates for their global minima.

VI. SUMMARY AND CONCLUSION

It has been shown that the *n*-body decomposition scheme works very well for the interaction and electron correlation energy of van der Waals–and hydrogen-bonded clusters. In the case of metallic or covalent interactions, the *n*-body decomposition converges very slowly. In particular, the 1D and 2D structures show large higher-order contributions, as the number of close neighbor two-body interactions is smaller, making it difficult to develop reliable many-body potentials.

The investigation of available interaction potentials for Au clearly shows that these have fast-converging characteristics, thus failing to reproduce the *ab initio* data: in the case of 1D and 2D structures, the potentials (with the exception of the Glue potential) favor lower-order interactions, whereas the *n*-body decomposition of the density functional and *ab initio* calculations show that the higher-order interactions are more important. The Glue potential exhibits very similar many-body characteristics for all different clusters, thereby giving good agreement for the low-dimensional structures but very poor agreement for the 3D structure. Empirical potentials often use parameters solely optimized to reproduce certain bulk material properties. Applying these potentials to small cluster systems appears at least doubtful. We question the validity of locating the global minimum for Au clusters using any of the investigated interaction potentials; see, e.g., Garzón *et al.* [68]. Including quantum mechanics at some stage becomes necessary for the description of Au clusters. The recent PM6 parametrization for the semiempirical MNDO method performs much better for all clusters investigated. This method should provide a computationally affordable way to obtain reliable cluster energies for Au and thus may constitute an efficient means of producing relevant structures for global minima searches.

The large contribution of higher-order many-body contributions is known for other systems such as HF oligomers [69], and this will make the development of accurate interaction potentials very difficult, if not impossible. We suggest that any new model developed for the simulation of larger clusters should be analyzed carefully using the *n*-body expansion.

ACKNOWLEDGMENTS

I.P.H. is grateful to Massey University for support from the International Visitor Research Fund. R.K. is grateful to the Alexander von Humboldt Foundation for support. This work was financed by a Marsden grant (No. MAU-313) through the Royal Society of New Zealand.

[1] R. Jaquet, in *Lecture Notes in Chemistry*, edited by A. F. Sax (Springer, Heidelberg, 1999), Vol. 71, p. 97.
[2] J. N. Murrell, S. Carter, S. Frantos, P. Huxley, and A. J. C. Varandas, *Molecular Potential Energy Functions* (Wiley, New York, 1984).
[3] J. E. Jones and A. E. Ingham, Proc. R. Soc. London, Ser. A **107**, 636 (1925).
[4] I. G. Kaplan, in *Handbook of Molecular Physics and Quantum Chemistry*, edited by Stephen Wilson (Wiley, New York, 2003), Vol. 3, p. 182.
[5] P. Schwerdtfeger, N. Gaston, R. P. Krawczyk, R. Tonner, and G. E. Moyano, Phys. Rev. B **73**, 064112 (2006).
[6] H. Shimizu, H. Tashiro, T. Kume, and S. Sasaki, Phys. Rev. Lett. **86**, 4568 (2001).
[7] P. M. Morse, Phys. Rev. **34**, 57 (1929).
[8] G. Bravo-Pérez, I. L. Garzón, and O. Novaro, J. Mol. Struct.: THEOCHEM **493**, 225 (1999).
[9] H. Häkkinen, M. Moseler, and U. Landman, Phys. Rev. Lett. **89**, 033401 (2002).
[10] A. P. Sutton and J. Chen, Philos. Mag. Lett. **61**, 139 (1990).
[11] F. Cleri and V. Rosato, Phys. Rev. B **48**, 22 (1993).
[12] R. P. Gupta, Phys. Rev. B **23**, 6265 (1981).
[13] P. Pyykkö, Angew. Chem., Int. Ed. **43**, 4412 (2004).
[14] P. Schwerdtfeger, Angew. Chem., Int. Ed. **42**, 1892 (2003).
[15] M. Haruta, Chem. Rec. **3**, 75 (2003).
[16] W. T. Wallace and R. L. Whetten, J. Am. Chem. Soc. **124**, 7499 (2002).
[17] N. Lopez and J. K. Nørskov, J. Am. Chem. Soc. **124**, 11262 (2002).
[18] S. Carretin, P. McMorn, P. Johnston, K. Griffin, C. J. Kiely, and G. J. Hutchings, Phys. Chem. Chem. Phys. **5**, 1329 (2003).
[19] G. C. Bond, Catal. Today, **72**, 5 (2002).
[20] A. Sanchez, S. Abbet, U. Heiz, W.-D. Schneider, H. Häkkinen, R. N. Barnett, and U. Landmann, J. Phys. Chem. A **103**, 9573 (1999).
[21] D. S. Cameron, Gold Bull. **36**, 17 (2003).
[22] C. W. Corti, R. J. Holliday, and D. T. Thompson, Gold Bull. **35**, 111 (2002).
[23] K. Kerman, Y. Morita, Y. Takamura, M. Ozsoz, and E. Tamiya, Anal. Chim. Acta **510**, 169 (2004).
[24] Á. G. Barrientos, J. M. de la Fuente, T. C. Rojas, A. Fernández, and S. Penadés, Chem.-Eur. J. **9**, 1909 (2003).
[25] C. L. Cheung, J. A. Camerero, B. W. Woods, T. Lin, J. E. Johnson, and J. J. De Yoreo, J. Am. Chem. Soc. **125**, 6848 (2003).
[26] H. Gu, P. L. Ho, E. Tong, L. Wang, and B. Xu, Nano Lett. **3**, 1261 (2003).
[27] T. Söhnel, H. Hermann, and P. Schwerdtfeger, Angew. Chem., Int. Ed. **40**, 4381 (2001).
[28] P. Schwerdtfeger and G. A. Bowmaker, J. Chem. Phys. **100**, 4487 (1994).
[29] P. Schwerdtfeger, R. P. Krawczyk, A. Hammerl, and R. Brown, Inorg. Chem. **43**, 6707 (2004).

[30] Y. Kondo and K. Takayanagi, Science **289**, 606 (2000).
[31] J. Li, X. Li, H.-J. Zhai, and L.-S. Wang, Science **299**, 864 (2003).
[32] J. Wang, G. Wang, and J. Zhao, Chem. Phys. Lett. **380**, 716 (2003).
[33] F. Ercolessi, M. Parrinello, and E. Tosatti, Philos. Mag. A **58**, 213 (1988).
[34] N. T. Wilson and R. L. Johnston, Eur. Phys. J. D **12**, 161 (2000).
[35] J. P. K. Doye and D. J. Wales, New J. Phys. **22**, 733 (1998).
[36] H. Cox, R. L. Johnston, and J. N. Murrell, J. Solid State Chem. **145**, 517 (1999).
[37] I. G. Kaplan, R. Santamaria, and O. Novaro, Mol. Phys. **84**, 105 (1995).
[38] A. V. Walker, J. Chem. Phys. **122**, 094310 (2005).
[39] H. Häkkinen, B. Yoon, U. Landmann, X. Li, H.-J. Zhai, and L.-S. Wang, J. Phys. Chem. A **107**, 6168 (2003).
[40] J. Wang, G. Wang, and J. Zhao, Phys. Rev. B **66**, 035418 (2002).
[41] M. Moseler, in *NIC Symposium 2004, NIC Series*, edited by D. Wolf, G. Münster, and M. Kremer (John von Neumann Institute for Computing, Jülich, 2003), Vol. 20, p. 181.
[42] M. J. Frisch *et al.*, Computer code Gaussian 03, revision C.02, Gaussian, Inc., Pittsburgh, PA, 2003.
[43] S. H. Vosko, L. Wilk, and M. Nusair, Can. J. Phys. **58**, 1200 (1980).
[44] A. D. Becke, J. Chem. Phys. **98**, 5648 (1993).
[45] J. P. Perdew, J. A. Chevary, S. H. Vosko, K. A. Jackson, M. R. Pederson, D. J. Singh, and C. Fiolhais, Phys. Rev. B **46**, 6671 (1992).
[46] C. Thierfelder, A. Hermann, P. Schwerdtfeger, and W. G. Schmidt, Phys. Rev. B **74**, 045422 (2006).
[47] D. E. Woon and T. H. Dunning, J. Chem. Phys. **98**, 1358 (1993).
[48] P. J. Hay and W. R. Wadt, J. Chem. Phys. **82**, 284 (1985).
[49] C. Jacob and P. Schwerdtfeger (unpublished).
[50] M. Grimsditch, P. Loubeyre, and A. Polian, Phys. Rev. B **33**, 7192 (1986).
[51] N. Gaston and P. Schwerdtfeger, Phys. Rev. B **74**, 024105 (2006).
[52] K. Rosciszewski, B. Paulus, P. Fulde, and H. Stoll, Phys. Rev. B **62**, 5482 (2000).
[53] E. C. Honea, A. Ogura, D. R. Peale, C. Felix, C. A. Murray, K. Raghavachari, W. O. Sprenger, M. F. Jarrold, and W. L. Brown, J. Chem. Phys. **110**, 12161 (1999).
[54] B. Hartke, Theor. Chem. Acc. **99**, 241 (1998).
[55] S. Li, R. J. van Zee, W. Weltner, and K. Raghavachari, Chem. Phys. Lett. **243**, 275 (1995).
[56] V. Bonacić-Koutecký, J. Burda, R. Mitrić, and M. Ge, J. Chem. Phys. **117**, 3120 (2002).
[57] O. Engkvist, P.-O. Astrand, and G. Karlstrom, Chem. Rev. (Washington, D.C.) **100**, 4087 (2000).
[58] M. P. Hodges, A. J. Stone, and S. S. Xantheas, J. Phys. Chem. A **101**, 9163 (1997).
[59] J. Kim, D. Majumdar, H. M. Lee, and K. S. Kim, J. Chem. Phys. **110**, 9128 (1999).
[60] I. G. Kaplan, J. Hernández-Cobos, I. Ortega-Blake, and O. Novaro, Phys. Rev. A **53**, 2493 (1996).
[61] H. Stoll (personal communication).
[62] H. Cox, X. Liu, and J. N. Murrell, Mol. Phys. **93**, 921 (1998).
[63] N. T. Wilson and R. L. Johnston, J. Mater. Chem. **12**, 2913 (2002).
[64] N. T. Wilson, Ph.D. thesis, University of Birmingham, 2000.
[65] Ş. Erkoç and Ş. Katircioğlu, Chem. Phys. Lett. **147**, 476 (1988).
[66] J. J. P. Stewart, PM6 code as implemented in MOPAC2007, version 7.072, Stewart Computational Chemistry, 2007, http://OpenMOPAC.net.
[67] J. J. P. Stewart, Computer code MOPAC2007, Stewart Computational Chemistry, 2007.
[68] I. L. Garzón, K. Michaelian, M. R. Beltrán, A. Posada-Amarillas, P. Ordejón, E. Artacho, D. Sánchez-Portal, and J. M. Soler, Phys. Rev. Lett. **81**, 1600 (1998).
[69] L. Rinón, R. Almeida, and D. G. Aldea, Int. J. Quantum Chem. **102**, 443 (2005).